Solid-State Graft Polymerization of Styrene in Spherical Polypropylene Particles in the Presence of Montmorillonite

Zhisheng Fu,[1] Fangli Sun,[1,2] Zhiqiang Fan[1]

[1]*Ministry of Education Key Laboratory of Macromolecular Synthesis and Functionalization, Department of Polymer Science and Engineering, Zhejiang University, Hangzhou 310027, China*
[2]*School of Engineering, Zhejiang Forestry University, Lin'an 311300, China*

Received 17 January 2011; accepted 5 November 2011
DOI 10.1002/app.36651
Published online in Wiley Online Library (wileyonlinelibrary.com).

ABSTRACT: In this work, cetyltrimethyl ammonium bromide and methacryloyloxyethyhrimethyl ammonium chloride were used to prepare organophilic montmorillonite (O-MMT). Then, polypropylene (PP)–clay nanocomposites were prepared by the *in situ* grafting polymerization of styrene (St)-containing O-MMT onto PP with *tert*-butyl perbenzoate as an initiator in the solid state. Fourier transform infrared spectroscopy, gel permeation chromatography, transmission electron microscopy, and X-ray diffraction were applied to study the structure of the layered silicate and modified PP. The surfaces of the composites and, thus, the distribution of the clay in the PP matrix were characterized by scanning electron microscopy. The rheology and mechanical properties were studied and are discussed. According to the characterization results, OMMT and St were already grafted onto the PP main chain. Also, the intercalated structure of montmorillonite could be stabilized, and a stable exfoliated structure could be attained. Namely, intercalated PP/OMMT nanocomposites were obtained. The rheological results clearly show that these PP/OMMT nanocomposites had long-chain-branched structures. The peroxide modification of PP had minor effects on the tensile and bending strengths of the modified PP; however, this modification resulted in a significant reduction in the impact strength. J Appl Polym Sci 000: 000–000, 2012

Key words: clay; graft copolymers; nanocomposites; polyolefins

INTRODUCTION

Polypropylene (PP) is a widely used polymer. However, for thermodynamic reasons, it is very incompatible with other polymers. Furthermore, its high surface energy and crystallinity make it difficult to adhere onto polymer or metal surfaces. Therefore, extensive research has been done on the chemical modification of this polyolefin. The grafting of PP with a vinyl monomer offers an effective approach for modifying its performance.[1–5] The grafting of PP can be carried out in the melt, in solution, or in the solid state. Solid-state grafting polymerization has many advantages, such as a lower required solvent amount, a lower required temperature, and a higher grafting degree.[6]

Polymer/clay nanocomposites have recently attracted increasing attention in academia and industry because of their significantly improved mechanical strength and stiffness, gas-barrier behavior, thermal, optical, and physicochemical properties, and so on.[7–9] For example, with as little as 2 vol % montmorillonite (MMT), nylon 6 nanocomposites can possess double the tensile strength and modulus of the parent polymer. Because MMT is hydrophilic, it is incompatible with most polymers. MMT is usually modified by alkyl ammonium groups to improve its compatibility with polymers. Meanwhile, the chemical modification of polyolefin resins with a polar monomer,[10–12] for example, the grafting of pendant anhydride groups, has become the main method for enhancing their miscibility with inorganic clay. Thus, polyolefin/clay nanocomposites can be prepared. Although compatibilizers and surface modifications have been used in the fabrication of nanocomposites, there is no guarantee of a strong bond between the compatibilizer and the clay surface. As a result, the crystallization of the PP matrix, which occurs quickly upon cooling, can lead to clay expulsion from the crystalline phase by thermodynamic forces.[13] In this study, cetyltrimethyl ammonium bromide (CTAB) and methacryloyloxyethyhrimethyl ammonium chloride (DMC) were the

Correspondence to: Z. Fan (fanzq@zju.edu.cn).
Contract grant sponsor: National Natural Science Foundation of China; contract grant number: 20874084.
Contract grant sponsor: Major State Basic Research Programs; contract grant number: 2005CB623804.
Contract grant sponsor: Seed Foundation for Interdiscipline of Zhejiang University.

alkyl ammoniums used in the preparation of organophilic montmorillonite (O-MMT). Their molecular structures are shown in Scheme 1. In particular, DMC had a reactive double bond that could copolymerize with styrene (St) to form poly(styrene-*co*-methacryloyloxyethyhrimethyl ammonium chloride). This copolymer acted as a bridge between the layers of MMT and PP. Thus, through the free-radical grafting polymerization of St-containing O-MMT onto PP in the solid phase, OMMT and St could be grafted onto the PP main chain. The rheology and mechanical properties of these graft copolymers were studied and are discussed.

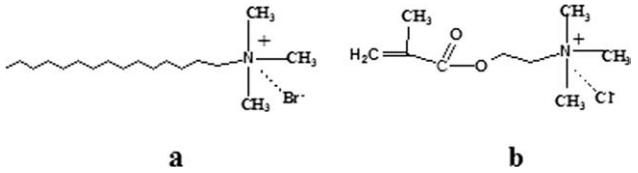

Scheme 1 Molecular structure of (a) CTAB and (b) methacryloyloxyethyltrimethyl ammonium chloride.

EXPERIMENTAL

Materials

Nascent PP particles (kindly donated by Sinopec Qilu Co., Ltd., Zibo, China) were used as the matrix for the grafting polymerization. The particles had a spherical shape with a diameter of 1.43–2.0 mm and a porosity of about 23%.

St (>98%) was purified by washing with 10% NaOH and then distilling under reduced pressure. *Tert*-Butyl perbenzoate (TBPB; Acros, Beijing, China) was used as the initiator without further purification. Sodium montmorillonite (Na-MMT) was kindly supplied by Zhejiang Fenghong Clay Chemicals Co., Ltd. (China). The cation-exchange capacity was about 90 mmol/100 g of MMT. CTAB and methacryloyloxyethyltrimethyl ammonium chloride (DMC; 75.1%) were purchased from Yinhu Chemical Co. (Hangzhou, Zhejiang, China).

Preparation of O-MMT

O-MMT was prepared by the cation-exchange reaction between Na^+ in the interlayer spaces of MMT and organoammonium cations in aqueous solution. An amount of 15 g of Na-MMT was suspended in 500 mL of distilled water and stirred for 2 h. The suspension was then heated to 70°C, and an aqueous solution of 20 mmol of CTAB or a mixture of 13.3 mmol of CTAB and 6.7 mmol of DMC was gradually added under stirring over 4 h. The organically exchanged MMTs were filtered and washed with distilled water until no bromide ion was detected with a 0.1*M* $AgNO_3$ solution. They were then dried *in vacuo* at 50°C. The organically modified clay was ground with a grinding mill and screened with a 200-mesh net. MMT modified by CTAB is referred to as CTAB–MMT. MMT modified by 13.3 mmol CTAB and 6.7 mmol DMC is referred to as 2C1D–MMT because the molar ratio between CTAB and DMC was equal to 2 : 1.

Preparation of the PP/O-MMT mixture

The PP/O-MMT mixtures, namely, PP/CTAB–MMT and PP/2C1D–MMT, were prepared as followed. PP (10 g) was first dissolved in 500 mL of xylene. Then, 0.1 g of CTAB–MMT or 2C1D–MMT was added to the solution. The mixture was heated under reflux and stirred vigorously for 2 h. Then, the solution was concentrated, and the resultant PP/O-MMT mixture was dried *in vacuo* at 60°C for 24 h.

The scaled-up preparation of the PP/O-MMT mixture was performed with 150 g of PP as the matrix. The resulting products were treated by the previous procedure and were then used as samples for the measurement of the mechanical properties.

Grafting polymerization of St onto PP in the presence of O-MMT

The grafting polymerization was carried out in a three-necked Schlenk flask equipped with a mechanical stirrer. PP particles (10.0 g) were charged into the reactor. After three thaw–vacuum treatments, a solution of 0.05 g of TBPB and a designated amount of O-MMT in 5.45 g of St were stirred for 30 min and then injected into the reactor *in vacuo* by a syringe. The reactor was then pressurized with nitrogen. The reactor was first stirred at 60°C for 1 h to ensure complete sorption of the liquid phase into the PP particles, then quickly moved into an oil bath set at 130°C, and stirred for 2 h to complete the grafting polymerization. The product, which was still in a spherical shape, was then washed with a mixture of ethanol and *n*-heptane to remove the residual St in the particles and then dried *in vacuo* for 24 h at 50°C. The resultant product of the grafting polymerization of St onto PP in the presence of CTAB–MMT is referred to as PP-*g*-polystyrene (PS)–CTAB–MMT. The resultant product of the grafting polymerization of St onto PP in the presence of 2C1D–MMT is referred to as PP-*g*-PS–2C1D–MMT.

The scaled-up grafting polymerization of St onto PP in the presence of O-MMT was performed with 150 g of PP as the matrix. The resultant products were treated by the previous procedure and were then used as samples for the measurement of the mechanical properties.

Measurements

Fourier transform infrared (FTIR) analysis was carried out with a Bruker Vector 22 infrared spectrometer (Karlsruhe, Germany). Thin films of the samples were prepared by hot compression molding at 190°C for about 10 s at 20 MPa. The grafting degree was determined by a procedure reported in the literature.[14,15]

The degree of grafting (DG) was defined as follows:

$$\mathrm{DG}(\%) = \frac{W_g}{W_g + W_{\mathrm{pp}}} \times 100\%$$

where W_g is the weight of PS grafted onto PP and W_{PP} is the weight of PP.

The interlayer spacing of the clay was studied by means of wide-angle X-ray diffraction (XRD) analysis, which was carried out at room temperature by a Rigaku D/max-γB diffractometer (Tokyo, Japan, 30 kV, 10 mA) with Cu Kα ($\lambda = 1.54$ Å) irradiation at a scanning rate of 8°/min in the range 0.5–40°.

The morphology and dispersion state of O-MMT in the PP matrix were investigated with a scanning electron microscope (JSM-T20, Tokyo, Japan). The scanning electron microscopy (SEM) samples were prepared as follows: strips of the polymer were prepared as described in the Mechanical Properties of the Composites section and were fractured in liquid nitrogen. Then, the fractured surface was coated with gold and observed by SEM.

The transmission electron micrographs were obtained with a JEM-1200EX electron microscope (Tokyo, Japan) to examine the dispersion and intercalation status of clay in the composites. The samples for transmission electron microscopy (TEM) observation were ultrathin-sectioned with a microtome equipped with a diamond knife. The sections (200–300 nm in thickness) were cut from a piece of about 1×1 mm^2, and they were collected in a trough filled with water and placed on a 200-mesh copper grid.

The molecular weight and its distribution were measured by gel permeation chromatography with a PL-220 gel permeation chromatograph (Wellesley, MA) (1,2,4-trichlorobenzene eluent, 150°C, PL mixed-B columns) with universal calibration on the basis of PS standards.

Rheological measurements

Before the measurements, the polymer samples were stabilized with 5000 ppm of Irganox 1010 antioxidant. Acetone, as a solvent for the stabilizer, was used to assist with the mixing of the powder of PP or the PP-*g*-PS copolymers. The solvent was evaporated *in vacuo* at 50°C overnight.

An ARES rotational rheometer (TA Instruments, New Castle, DE) was used to measure the complex modulus and complex viscosities of the PP and PP-*g*-PS copolymers. The frequency range was 0.01–100 s^{-1}, and the temperature was 190°C. Measurements of the dynamic viscosity were performed with a parallel-plate fixture (diameter = 25 mm) with a gap distance of 2.5 mm, and the strain was kept at 10% to ensure linear viscoelasticity. The measurements were conducted under a nitrogen atmosphere to prevent degradation.

Mechanical properties of the composites

The notched Charpy impact strength of the polymer sample was measured on a Ceast impact strength tester according to ASTM D 256-2006. The flexural modulus was measured following ASTM D 790-07 on a Shimadzu AG-500A electronic tester (Kyoto, Japan). The polymer particles were heat-molded at 170°C into sheets, which were then cut into pieces, put into a $150 \times 100 \times 4$ mm^3 mold, and pressed under 14.5 MPa at 180°C for 5 min. The sample plates were then slowly cooled to room temperature in the mold. Sample strips for the tests were cut from the plate following ASTM standards. For each test point, five parallel measurements were made, and the average values were adopted.

RESULTS AND DISCUSSION

FTIR spectra of the MMT, O-MMTs, and modified PP

With 0.05 g of TBPB as the initiator, 1 g of O-MMT (CTAB–MMT or 2C1D–MMT) dissolved in 5.45 g of St was grafted onto 10 g of PP particles at 130°C for 2 h. The resultant products were PP-*g*-PS–2C1D–MMT and PP-*g*-PS–CTAB–MMT, respectively. Figure 1 shows the FTIR spectra of Na-MMT, CTAB–MMT, 2C1D–MMT, PP-*g*-PS without O-MMT, PP-*g*-PS–2C1D–MMT, and PP-*g*-PS–CTAB–MMT. The grafting degrees of PP-*g*-PS (without O-MMT), PP-*g*-PS–2C1D–MMT, and PP-*g*-PS–CTAB–MMT were 12.8, 13.1, and 11.4%, respectively. As shown in Figure 1(a), Na-MMT had characteristic absorptions at 3625, 3410, 3200, and 1030 cm^{-1}, which were attributed to the O—H vibration, the intermolecular hydrogen bonding between the stacked silicate sheets, and Si—O stretching, respectively. After Na-MMT was ion-exchanged with CTAB or the mixture of CTAB and DMC, the absorption of the intermolecular hydrogen bonding declined because the layer spacing of MMT was expanded. In the spectra of O-MMTs [Fig. 1(b,c)], the bands at 2925, 2852, 1475, and 725 cm^{-1} were attributed to C—H vibrations. Compared with the spectrum of CTAB–MMT, a

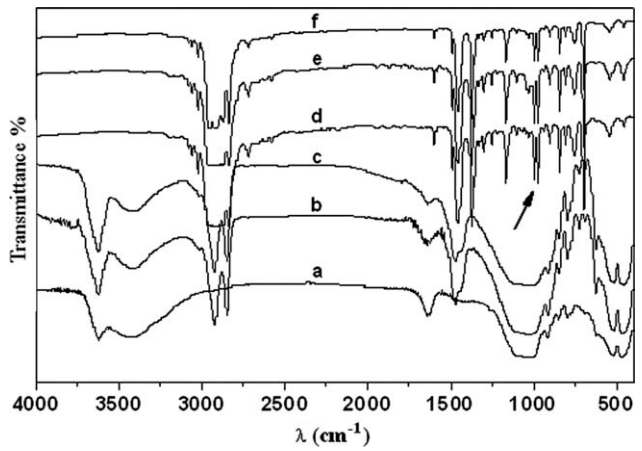

Figure 1 FTIR spectra of (a) Na-MMT, (b) CTAB–MMT, (c) 2C1D–MMT, (d) PP-*g*-PS without O-MMT, (e) PP-*g*-PS–2C1D–MMT, and (f) PP-*g*-PS–CTAB–MMT.

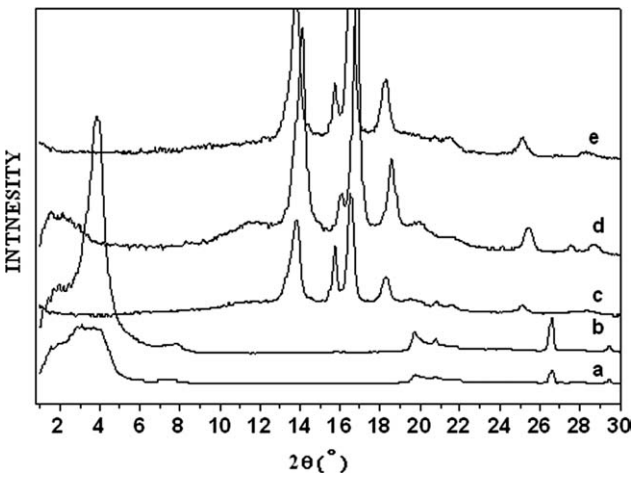

Figure 2 XRD patterns of (a) CTAB–MMT, (b) 2C1D–MMT, (c) PP-*g*-PS–2C1D–MMT, (d) PP-*g*-PS–CTAB–MMT, and (e) PP-*g*-PS.

small peak at 1794 cm^{-1}, associated with the stretching vibrations of C=O in DMC, was observed in the spectrum of 2C1D–MMT. This indicated that DMC was attached to MMT. Compared with those of PP-*g*-PS [Fig. 1(d)], those peaks centered at 1030 cm^{-1} in the spectra of PP-*g*-PS–2C1D–MMT and PP-*g*-PS–CTAB–MMT became deformed and broadened because of the overlapping of MMT in the same regions.

XRD of the O-MMTs and modified PP

As listed in Table I, the basal spacing (d_{001}) values of Na-MMT and O-MMT from the XRD measurement were calculated at peak positions according to Bragg's law:

$$d_{001} = \lambda/(2\sin\theta)$$

where θ is the diffraction angle and d_{001} of Na-MMT is 1.523 nm. In CTAB–MMT and 2C1D–MMT, the d_{001} values increased to 2.884 and 2.264 nm, respectively.

The XRD patterns of CTAB–MMT, 2C1D–MMT, PP-*g*-PS–2C1D–MMT, PP-*g*-PS–CTAB–MMT, and PP-*g*-PS are shown in Figure 2. Reflection 110 (at 2θ = 14.11°), reflection 300 (at 2θ = 15.7–16.1°), reflection 040 (at 2θ = 16.9°), reflection 120 (at 2θ = 21.69°), and reflection 130 (at 2θ = 18.52°) in the XRD patterns of PP-*g*-PS–2C1D–MMT, PP-*g*-PS–CTAB–MMT, and PP-*g*-PS were from PP.[16] The intraplanar reflections (at 2θ = 19.7°) from the clay sheets were seen in both the pure organoclay and the composites. This indicated that the clay sheets stayed intact during the intercalation or exfoliation. In the pure organoclay, the clay sheets were separated by an interlayer distance (d_{001}). This spacing was responsible for the reflection 001 (at 2θ = 4.69°). For some of the composites, the reflection 001 moved to a smaller angle (curve d). This indicated that the clay in this sample was intercalated. In curve c, the reflection 001 disappeared completely; this indicated that its clay was exfoliated.

TABLE I
d_{001} Values of the Na-MMT and O-MMTs

Item	Na-MMT	CTAB–MMT	2C1D–MMT
2θ (°)	5.796	2.559	3.917
d_{001} (nm)	1.523	2.884	2.264

Morphology

In most cases, TEM combined with XRD confirmed the microstructure of the obtained nanocomposites, and it directly showed the dispersion of O-MMT in the PP matrix. Figure 3 shows the TEM imagines of the PP-*g*-PS–O-MMTs and the PP/O-MMT mixture, in which the dark regions indicate the layers of MMT.

As expected from the XRD results, the TEM images show the nanosized organoclay particles evenly dispersed in the PP matrix [Fig. 3(b–d)]. When O-MMT was just simply mixed with PP, O-MMT could not be dispersed evenly in the matrix, and microsize particles were present [Fig. 3(a)].

Figure 4 shows the SEM images of the fractured surfaces of the neat PP and composites, in which the light regions are the layers of MMT. The fractured surface of the neat PP [Fig. 4(a)] was smooth. There was little change in the surface structure when PP was simply mixed with 3 wt % (to the weight of PP) organoclay [Fig. 4(b)]. The organoclay particles could be clearly seen in the mixture. However, as already shown in the XRD and TEM images, various nanostructures formed in the PP-*g*-PS–O-MMT samples,

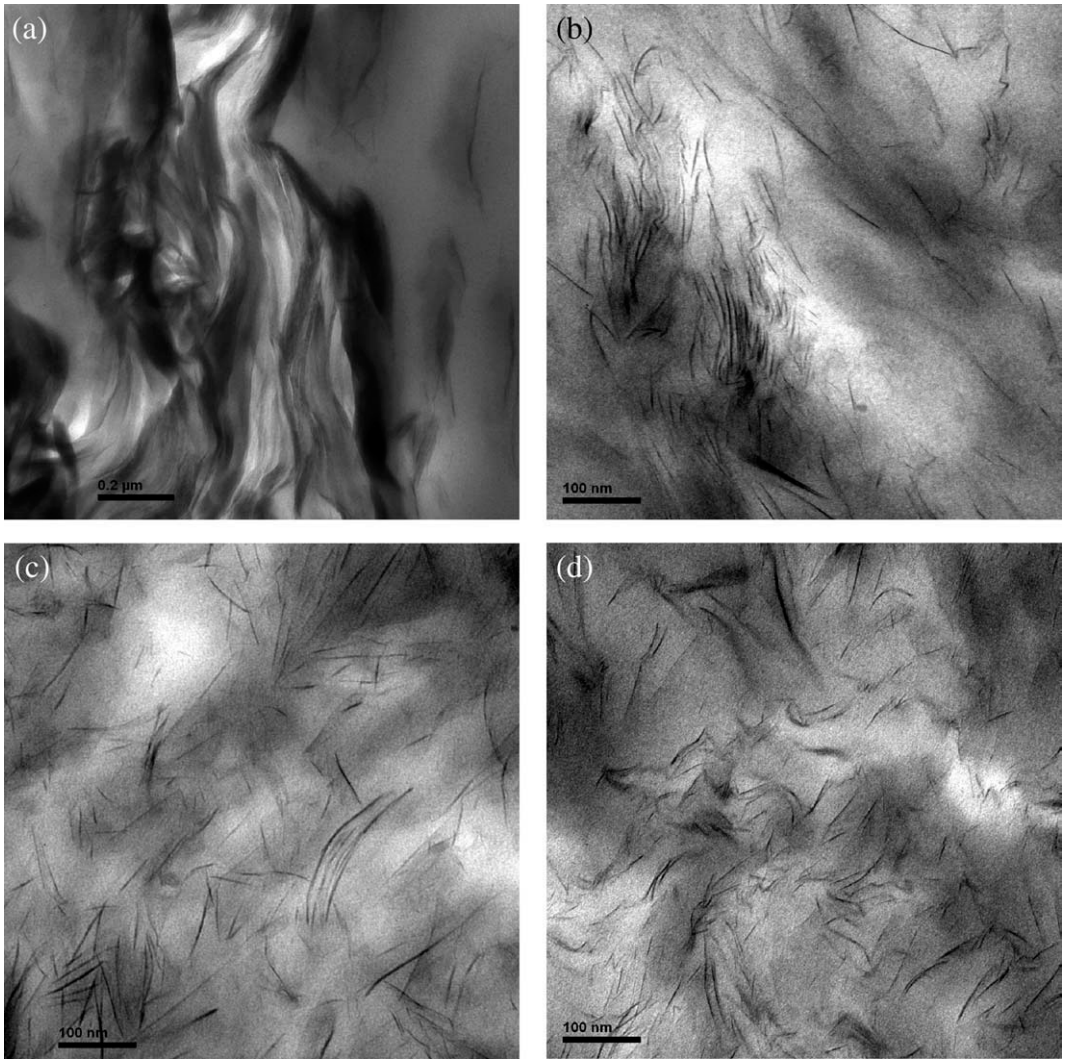

Figure 3 TEM images of (a) the mixture of PP and 2C1D–MMT, (b) PP-*g*-PS–CTAB–MMT (CTAB–MMT/PP = 1 wt %), (c) PP-*g*-PS–2C1D–MMT (2C1D–MMT/PP = 1 wt %), and (d) PP-*g*-PS-2C1D–MMT (2C1D–MMT/PP = 3 wt %).

and the different nanostructures affected the fractured surface. Compared with those of the neat PP and the mixture of O-MMT/PP, the fractured surfaces of PP-*g*-PS–O-MMT became rough, and the particle size of O-MMT in PP-*g*-PS–O-MMT decreased. More importantly, the exfoliation of the O-MMT layers could be clearly observed, and this confirmed the XRD results.

Influence of O-MMT on the molecular weight and polydispersity of the modified PP

The effect of O-MMT on the molecular weight distribution of PP-*g*-PS is shown in Table II. In general, during the peroxide modification of PP, two processes may take place simultaneously: a decrease in various labile bonds and an increase in the concentration of more reactive crosslinking centers in the macromolecules.[17] The former leads to a decrease in the molecular weight, whereas the latter leads to an increase in the molecular weight. The degree of degradation and/or crosslinking of PP depends on the amount of peroxide decomposed. In this work, we found that the molecular weight of PP-*g*-PS–CTAB–MMT [weight-average molecular weight (M_w) = 17.2 $\times$ 10^4] was similar to that of PP-*g*-PS (M_w = 16.0 $\times$ 10^4) but lower than that of the neat PP (M_w = 24.2 $\times$ 10^4). It is said during grafting polymerization, the degradation reactions of PP prevail. However, the molecular weights of the PP-*g*-PS–2C1D–MMTs were higher than those of PP-*g*-PS–CTAB–MMT. When the amount of 2C1D–MMT was 1 wt %, the molecular weight of PP-*g*-PS–2C1D–MMT was even close to that of the neat PP. However, the polydispersity was broadened to some extent. Because there were reactive double bonds in 2C1D–MMT, 2C1D–MMT could copolymerize with St to form poly(styrene-*co*-methacryloyloxyethyhrimethyl ammonium chloride). This copolymer acted as a bridge between the layers of MMT and PP. Thus, the copolymers and MMTs

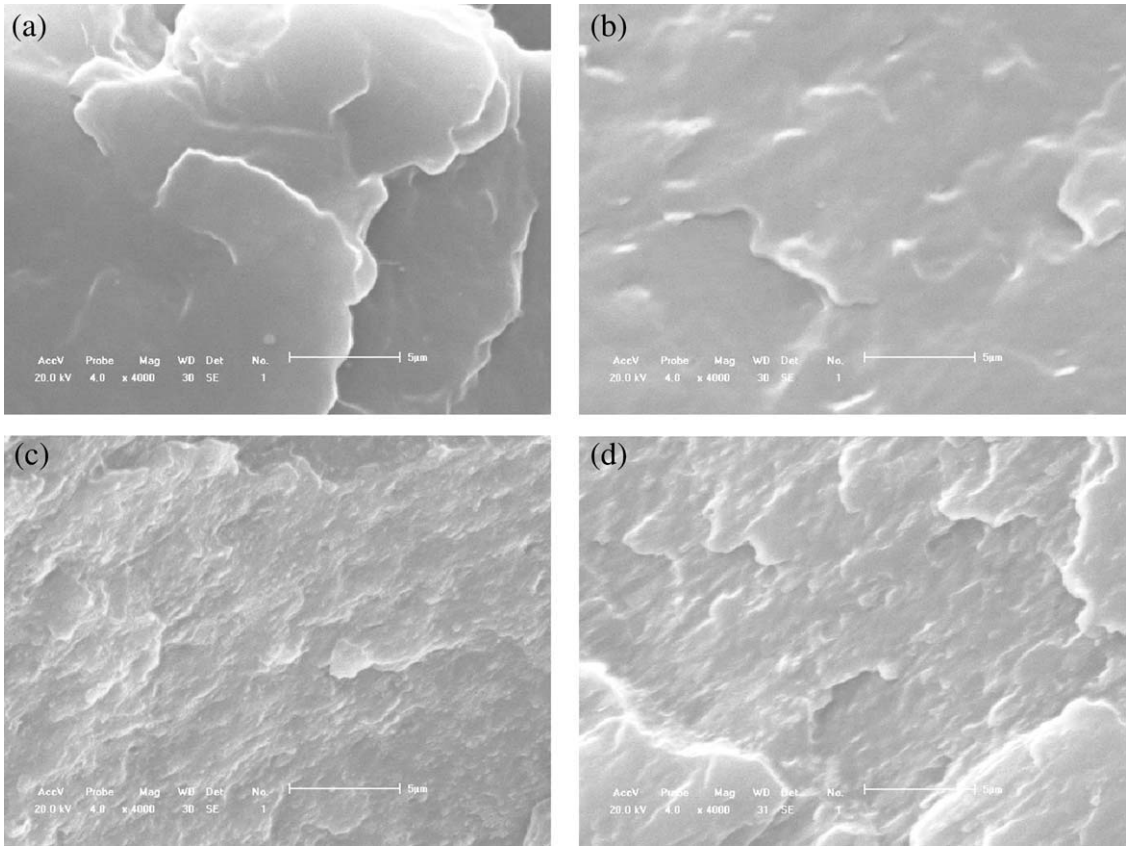

Figure 4 SEM images of the fracture surfaces of (a) PP, (b) the mixture of PP and 2C1D–MMT, (c) PP-*g*-PS–CTAB–MMT (CTAB–MMT/PP = 1 wt %), and (d) PP-*g*-PS–2C1D–MMT (2C1D–MMT/PP = 3 wt %).

became pendants on the PP backbone. This resulted in an increase in the molecular weight. However, because of the prevailing degradation reaction of PP, there were many PP fragments with relatively low molecular weights in PP-*g*-PS–2C1D–MMT. As a result, the polydispersity of PP-*g*-PS–2C1D–MMT was broadened.

Rheology

From the viewpoint of processing, a rheological study of polymer/clay nanocomposites is very crucial for predicting their processibility.[18–20] The melt rheological properties are crucially dependent not only on the strength of the polymer/organically modified layered silicate interaction but also on the inherent viscoelastic properties of the matrix in which the layers or collection of layers are dispersed.[21]

The dynamic linear viscoelastic behaviors of the samples in the melt state were examined in a constant-strain rheometer in a parallel-plate geometry. The linear viscoelastic responses, such as the storage modulus (G') and loss modulus (G''), for PP and the PP/O-MMTs composites are shown in Figure 5. It is known that G' and G'' represent the elastic and viscous responses of a controlled system, respectively. Both G' and G'' increased in all frequency regions for the PP/O-MMTs compared with PP. Both G' and G'' of PP-*g*-PS–2C1D–MMT were higher than those of PP-*g*-PS–CTAB–MMT. This indicated that MMT was dispersed better in PP-*g*-PS–2C1D–MMT than in PP-*g*-PS–CTAB–MMT.

As shown in Figure 5(a,b), in cases of PP-*g*-PS–2C1D–MMT and PP-*g*-PS–CTAB–MMT, Log G' was always higher than Log G'' in the whole range of frequencies studied. Additionally, at low frequencies,

TABLE II
Influence of O-MMT on the Molecular Weight and Polydispersity of the Modified PP[a]

Sample	Amount of O-MMT (wt %)[b]	M_n ($\times 10^{-4}$)	M_w ($\times 10^{-4}$)	M_w/M_n
PP-*g*-PS–2C1D–MMT	0.5	4.5	19.6	4.4
	1	3.8	24.8	6.5
	2	5.2	22.4	4.3
	3	4.6	17.1	3.7
PP-*g*-PS–CTAB-MMT	1	4.0	17.2	4.3
PP-*g*-PS	0	4.3	16.0	3.7
PP	0	5.4	24.2	4.5

M_n, number-average molecular weight.
[a] Polymerization conditions: TBPB/PP = 0.5 wt %, St/PP = 54.5 wt %, temperature = 130°C, and time = 2 h.
[b] Amount of O-MMT = weight percentage between O-MMT and PP.

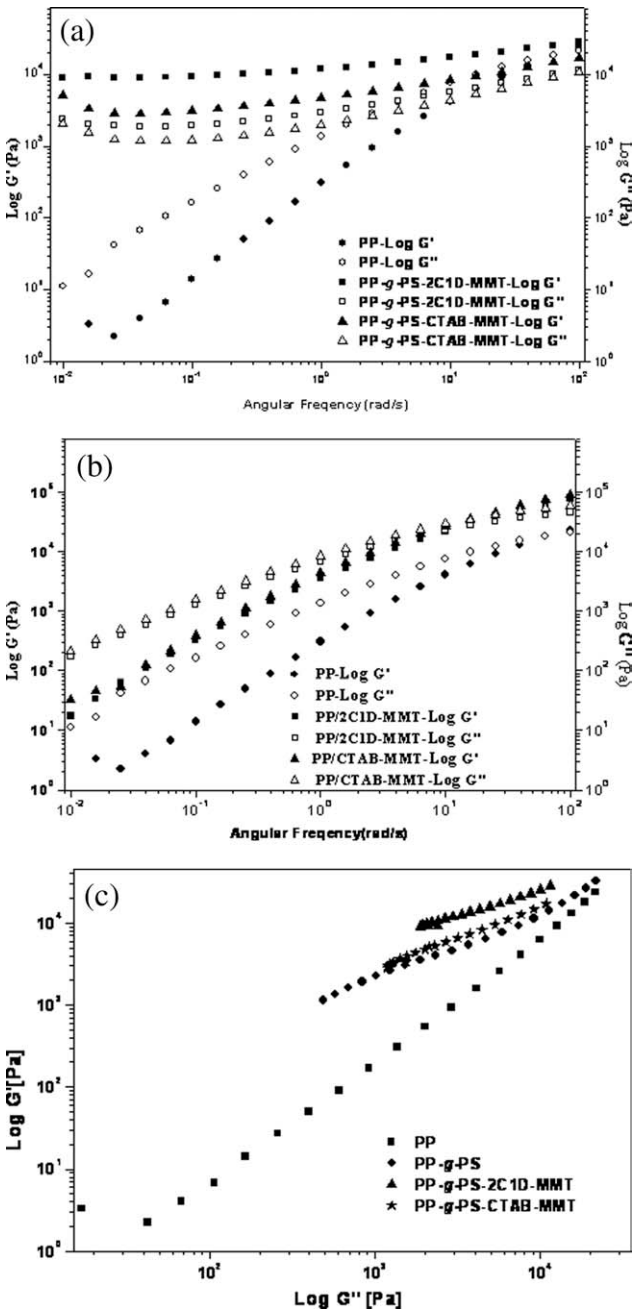

Figure 5 Log G' and Log G'' of PP, PP-*g*-PS, and PP-*g*-PS/O-MMTs measured at 200°C.

an upshift and a plateau behavior could be observed; this was significantly different from the behaviors of the neat PP and PP/O-MMTs. Similar changes have been observed in other studies.[22–24] This suggested that long-chain branched polymers were probably formed. The upshift behavior of PP-*g*-PS–2C1D–MMT was more significant than that of PP-*g*-PS–CTAB–MMT and indicated that there were more long-chain branches in PP-*g*-PS–2C1D–MMT. The Log G' versus log G'' plot has been proven to be a useful tool for investigating the effects of long-chain branching on the rheological properties.[25] Figure 5(c) presents the Log G' versus log G'' plots for PP, PP-*g*-PS and PP-*g*-PS–OMMT. PP-*g*-PS–2C1D–MMT and PP-*g*-PS–CTAB–MMT showed highly elastic behavior at low frequencies, whereas PP had no plateau behavior, and its plot lay in a straight line. These rheological results clearly show that PP-*g*-PS–2C1D–MMT and PP-*g*-PS–CTAB–MMT had long-chain-branched structures.

Mechanical properties

As shown in Table III, the peroxide modification of PP exerted minor influences on the tensile and bending strengths of the modified PP. However, the peroxide modification of PP resulted in a significant reduction in the impact strength. The impact strength of PP-*g*-PS, PP-*g*-PS–2C1D–MMT, and PP-*g*-PS–CTAB–MMT was just half of that of PP, PP/2C1D–MMT, and PP/CTAB–MMT. At the same time, the elongation at break of PP-*g*-PS, PP-*g*-PS–2C1D–MMT, and PP-*g*-PS–CTAB–MMT dropped significantly in comparison with PP, PP/2C1D–MMT, and PP/CTAB–MMT. This could be attributed to the degradation reactions of PP during the grafting polymerization. Moreover, the presence of PS lateral chains, which were more brittle than PP, could have been another factor.

CONCLUSIONS

In this article, OMMTs were introduced into an *in situ* solid-phase graft copolymerization to stabilize the intercalated structure of MMT and to achieve a stable exfoliated structure. FTIR analysis showed that OMMT and St were already grafted onto the PP main chain. XRD and TEM analyses indicated that intercalated PP/OMMT nanocomposites were obtained. The rheological results clearly show that

TABLE III
Mechanical Properties of the PP, PP-*g*-PS, and PP-*g*-PS/O-MMTs

Sample	PP	PP/2C1D–MMT	PP/CTAB–MMT	PP-*g*-PS	PP-*g*-PS–2C1D–MMT	PP-*g*-PS–CTAB–MMT
Tensile strength (MPa)	38.4	36.7	37.9	39.0	40.0	38.3
Bending strength (MPa)	48.4	44.0	44.4	49.4	53.0	46.0
Impact strength (kJ/m^2)	2.21	2.46	2.48	1.17	1.21	1.13
Elongation at break (%)	15.8	15.9	10.9	0.6	0.4	1.1

these PP/OMMT nanocomposites had long-chain-branched structures. The peroxide modification of PP had minor influences on the tensile and bending strengths of the modified PP. However, it resulted in a significant reduction in the impact strength.

References

1. Chapiro, A. J Polym Sci 1960, 48, 109.
2. Boutevin, B.; Robin, J. J.; Torres, N.; Casteil, J. Macromol Chem Phys 2002, 203, 245.
3. Boutevin, B.; Robin, J. J.; Torres, N.; Casteil, J. Polym Eng Sci 2002, 42, 78.
4. Boutevin, B.; Robin, J. J.; Serdani, A. Eur Polym J 1992, 28, 1507.
5. Boutevin, B.; Pietrasanta, Y.; Taha, M.; Sarraf, T. Eur Polym J 1984, 20, 875.
6. Ratzsch, M.; Arnold, M.; Borsig, E.; Bucka, H.; Reichelt, N. Prog Polym Sci 2002, 27, 1195.
7. Effenberger, F.; Schweizer, M.; Mohamed, W. S. Polym Plast Technol Eng 2010, 49, 525.
8. Yi, D. Q.; Yang, R. J. J Appl Polym Sci 2010, 118, 834.
9. Strecka, Z.; Ujhelyiova, A.; Bolhova, E.; Alexy, P.; Borsig, E. J Text Inst 2010, 101, 315.
10. Gopakumar, T. G.; Lee, J. A.; Kontopoulou, M.; Parent, J. S. Polymer 2002, 43, 5483.
11. Liang, G. D.; Xu, J. T.; Bao, S. P.; Xu, W. B. J Appl Polym Sci 2004, 91, 3974.
12. Ristolainen, N.; Vainio, U.; Paavola, S.; Torkkeli, M.; Serimaa, R.; Seppala, J. J Polym Sci Part B: Polym Phys 2005, 43, 1892.
13. Ton-That, M. T.; Leelapornpisit, W.; Utracki, L. A.; Perrin-Sarazin, F.; Denault, J.; Cole, K. C.; Bureau, M. N. Polym Eng Sci 2006, 46, 1085.
14. Deng, Q. T.; Fu, Z. S.; Zhang, L. T.; Xu, J. T.; Fan, Z. Q. e-Polymers 2006, 061, 1.
15. Sun, F. L.; Fu, Z. S.; Deng, Q. T.; Fan, Z. Q. J Appl Polym Sci 2009, 112, 275.
16. Selver, E.; Adanur, S. J Ind Text 2010, 40, 123.
17. Lazar, M.; Hrckova, L.; Borsig, E.; Marcincin, A.; Reichelt, N.; Ratzsch, M. J Appl Polym Sci 2000, 78, 886.
18. Gahleiner, M.; Kretzschmer, B.; Pospiech, D.; Ingolic, E.; Reichelt, N.; Bernreitner, K. J Appl Polym Sci 2006, 100, 283.
19. Hyun, Y. H.; Lim, S. T.; Choi, H. J.; Jhon, M. S. Macromolecules 2001, 34, 8084.
20. Gelfer, M. Y.; Burger, C.; Chu, B.; Hsiao, B. S.; Drozdov, A. D.; Si, M.; Rafailovich, M.; Sauer, B. B.; Gilman, J. W. Macromolecules 2005, 38, 3765.
21. Zhang, X.; Yang, G.; Lin, J. J Polym Sci Part B: Polym Phys 2006, 44, 2161.
22. Hingmann, R.; Marczinke, B. L. J Rheol 1994, 38, 573.
23. Malmberg, A.; Kokko, E.; Lehmus, P.;Löfgren. B. Seppälä, J. V. Macromolecules 1998, 31, 8448.
24. Villar, M. A.; Failla, M. D.; Quijada, R.; Mauler, R. S.; Valles, E. M.; Galland, G. B.; Quinzani, L. M. Polymer 2001, 42, 9269.
25. Vega, J. F.; Santamaria, A.; Munoz-Escalona, A.; Lafuente, P. Macromolecules 1998, 31, 3639.